GSNL - Geohazard Supersites and Natural Laboratories

Biennial report for Candidate/Permanent Supersite

Hawai'i Supersite

Annex to 2014–2016 report

Introduction

During 2014–2016, the Hawai'i Supersite achieved a number of noteworthy results. This annex details some of the more unique of those results in an effort to highlight how remote sensing data, particularly SAR, have been used to elucidate volcanic processes that might otherwise be obscured. For example, cross-polarized SAR amplitude imagery were critical for tracking lava flow activity in forested areas (co-polarized imagery could not distinguish forest from lava) and, when combined with coherence information, provided a means of mapping lava flow activity during the 2014–2015 Pāhoa lava flow crisis. Mauna Loa volcano—the largest active volcano in the world—began to inflate in 2014, with the locus of inflation changing over time (a variation that was identified by GPS but required InSAR to map fully). In September 2015, a pit crater formed unexpectedly near the summit access road of Mauna Kea volcano (which is not typically monitored by SAR and has few ground-based instruments), and opportunistic SAR acquisitions helped to constrain the crater's formation time and also detect pre-collapse subsidence. An intrusion of magma into the south part of Kīlauea Volcano in May 2015 was imaged in exceptional spatial and temporal detail thanks to ground-based continuous tilt and GPS coupled with InSAR results from several satellites. Finally, the combination of lava effusion rates derived from TanDEM-X and subsurface magma storage rates from multiple SAR satellites suggests that magma supply to Kīlauea increased in 2016, implying increased potential for future changes in eruptive activity as the volcano becomes engorged with magma.

Based on this record of achievement, the Hawai'i Supersite requests continued support with similar quotas of TerraSAR-X and Cosmo-SkyMed imagery (roughly 60 scenes/year and 150 scenes/year, respectively). In addition, a new allocation of RADARSAT-2 data is requested. The RADARSAT-2 quota was expended in 2015. Because those data are the longest current continuous C-band record of surface change of Hawaiian volcanoes and have quad-pol and very high resolution modes, they provide a unique perspective on deformation and lava flow emplacement in Hawai'i. The opportunistic RADARSAT-2 acquisitions also cover portions of the island not imaged by other SAR satellites, and therefore can be used to investigate processes occurring away from the summits and rift zones of Kīlauea and Mauna Loa volcanoes.

GSNL - Geohazard Supersites and Natural Laboratories

Lava flow mapping

Surface change due to the emplacement of volcanic deposits in unvegetated areas can be tracked with ease via interferometric coherence between SAR images acquired at different times. Vegetation is typically also incoherent (except in L-band SAR imagery), however, so change detection in forested areas using coherence is not possible. Amplitude imagery offers a potential means of overcoming this challenge, but backscatter differences between volcanic deposits and vegetation are small in co-polarized data (Figure 1, left), which is unfortunately the default acquisition mode for most SAR satellites. This challenge can be overcome by using cross-polarized SAR amplitude, as these images emphasize difference between vegetation and, for example, lava flows (Figure 1, right). RADARSAT-2 data are frequently acquired in high-resolution quad-pol modes, providing exceptional views of lava flow emplacement in forested areas—for example, during the 2014–2015 Pāhoa lava flow crisis at Kīlauea Volcano, when lava nearly overran a village on the eastern tip of the Island of Hawai‘i. By combining cross-polarized amplitude imagery from two different dates with the interferometric coherence across these dates in a 3-band (R-G-B) image, it is possible to achieve a high-spatial-resolution map of surface change due to volcanism regardless of ground cover (Figure 2). Such maps can be made regularly using cross-pol SAR data from both RADARSAT-2 and Sentinel-1a/b (Figure 3), and they are an invaluable complement to ground- and air-based mapping by the U.S. Geological Survey's Hawaiian Volcano Observatory. In fact, operational use of this method provides a new, all-weather, day/night tool for mapping volcanic deposits and assessing their hazards and impacts.

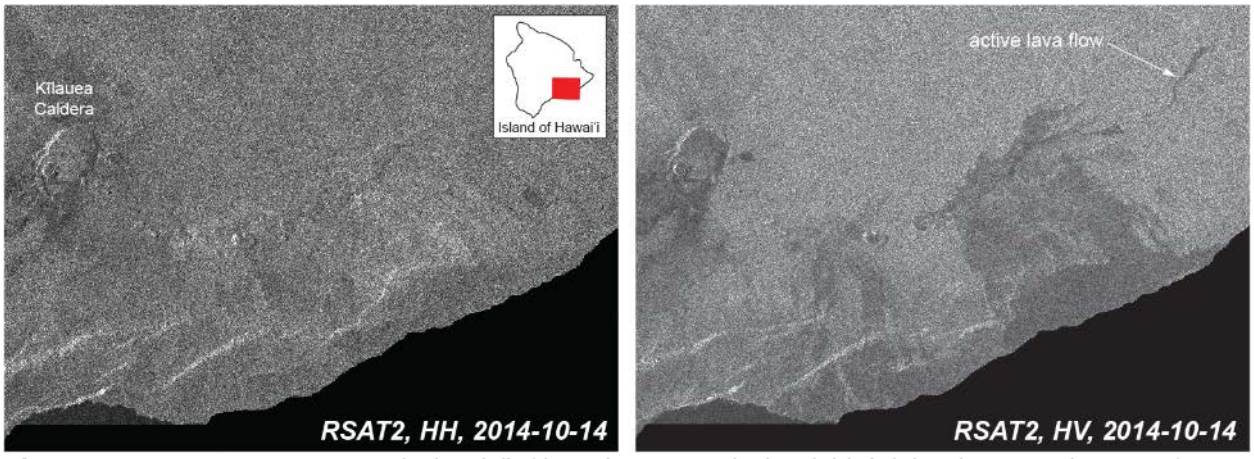

Figure 1. RADARSAT-2 co-polarized (left) and cross-polarized (right) backscatter images from Kīlauea Volcano. Both images are from the same acquisition. The active lava flow on the volcano's East Rift Zone can only be distinguished in the cross-polarized data.

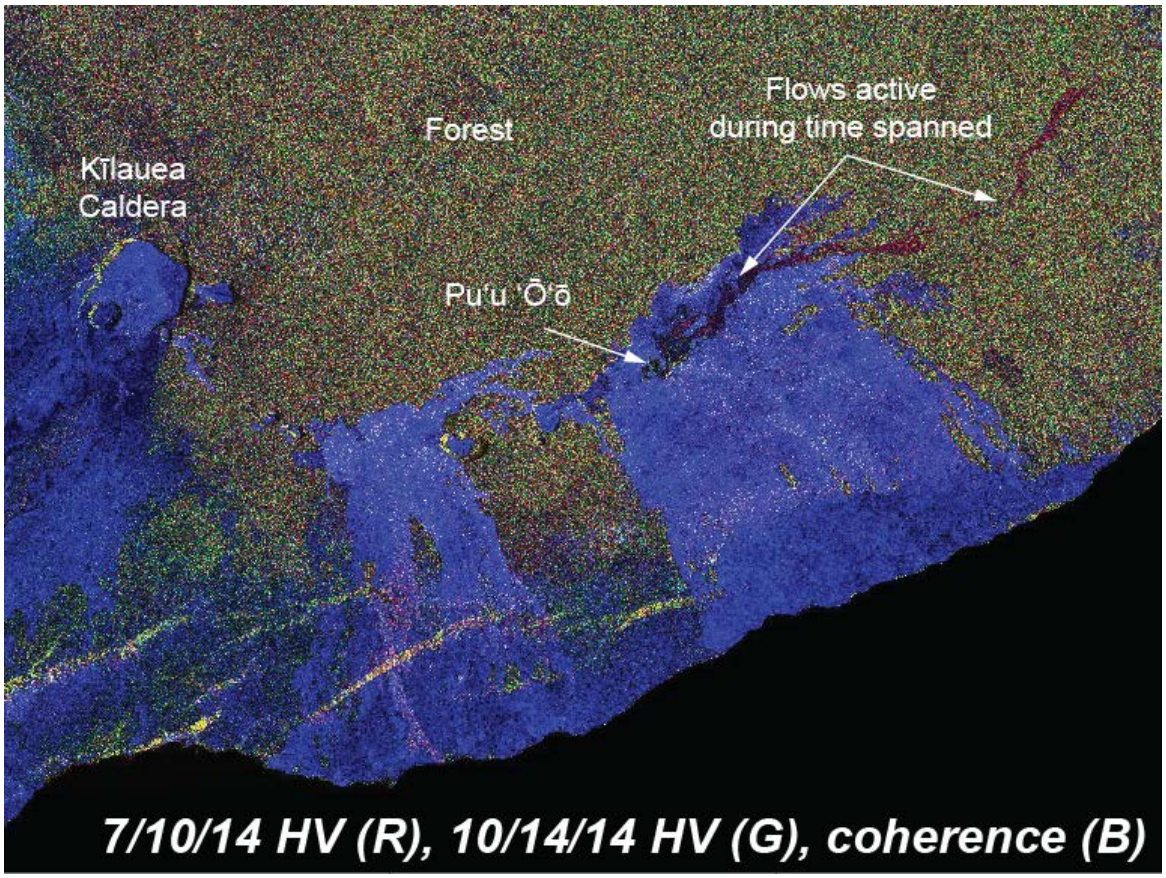

Figure 2. This false-color image integrates RADARSAT-2 cross-polarized (HV) data from July 10, 2014 (red), and October 14, 2014 (green), with a coherence map spanning the two time periods (blue). Flows that were active in forested areas during the time spanned appear red, while lava that covered older, unvegetated flows between the two time periods appears black. The combined cross-polarized and coherence imagery provides a complete view of lava flow activity over the time spanned, regardless of the type of ground that was covered by the lava. At the time the second image was acquired, this flow was threatening the village of Pāhoa.

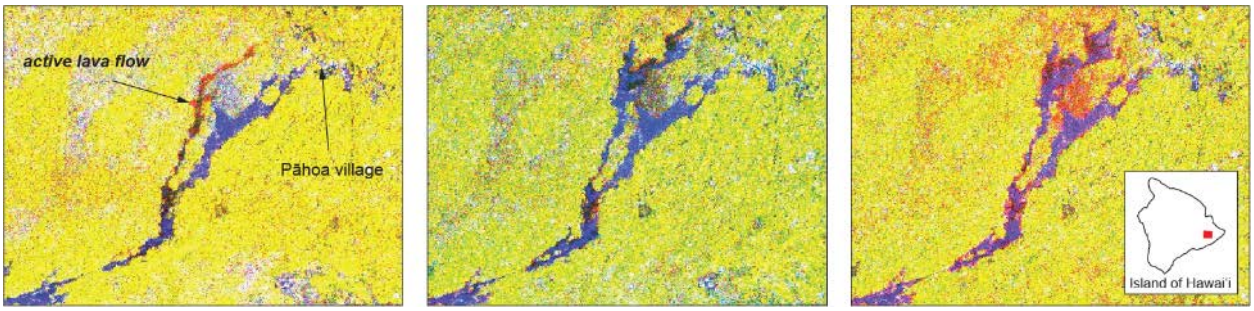

Figure 3. Sequential false-color images (R=earlier HV, G=later HV, B=coherence) from Sentinel-1a showing development of the Pāhoa lava flow field at Kīlauea Volcano, Hawai'i, during late 2014 and early 2015. Each image is approximately 10 km across. New lava flow activity appears reddish.

GSNL - Geohazard Supersites and Natural Laboratories

Deformation of Mauna Loa volcano

Mauna Loa—the largest active volcano on Earth—is currently experiencing the longest period of repose in the past ~200 years, having last erupted in 1984. The volcano is far from quiescent, however, with episodes of inflation and heightened seismicity testifying to the accumulation of magma beneath the volcano's summit. The most recent episode of inflation began in mid-2014, as indicated by continuous GPS data from the volcano's summit region (Figure 4, top). The deformation has been well-characterized by InSAR—especially Cosmo-SkyMed data—and through late 2014 and early 2015 resembled the previous period of inflation (Figure 5, upper left), which occurred during 2002–2009 and was centered on the southwest part of Mauna Loa's summit caldera. The deformation pattern suggested magma accumulation in a reservoir that was elongated along the length of the caldera and upper part of the volcano's south rift zone. In late 2015, GPS stations to the southeast of the summit began recording accelerated rates of deformation (Figure 4, bottom), while summit GPS stations showed a stalling in the inflation (Figure 4, top). Examination of InSAR results from Cosmo-SkyMed revealed that the inflation pattern had shifted to the southwest, suggesting that magma accumulation was occurring beneath the south rift zone only, and not beneath the summit (Figure 5, upper right and lower left). Such a pattern had never before been observed. By late 2016, however, the original pattern of inflation had reestablished itself, with deformation centered on the southwest part of the caldera (Figure 5, lower right). The mechanism and consequences of this shift on the locus of deformation is not clear, but suggests a complex magma plumbing system that is composed of compartments that can become isolated from one another.

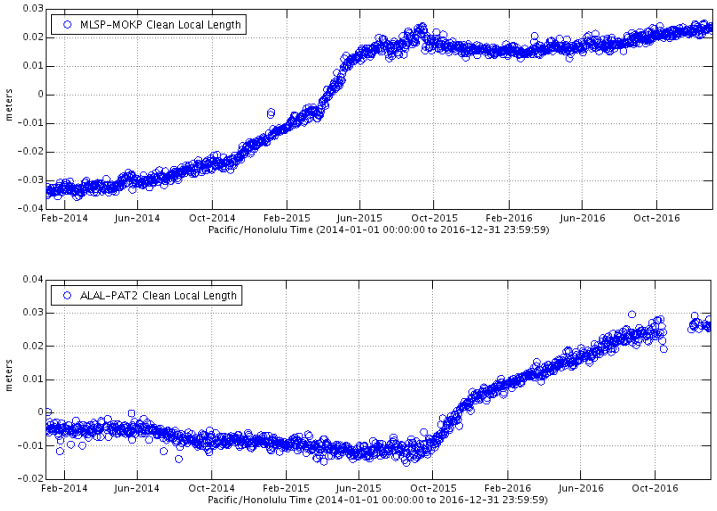

Figure 4. Distance change between GPS stations spanning the summit (top) and south rift zone (bottom) of Mauna Loa. Positive change is an increase in distance between stations, implying inflation due to subsurface magma accumulation. Inflation began at the summit in mid-2014, shifted to the southwest in late 2015, and returned to the summit area in late 2016.

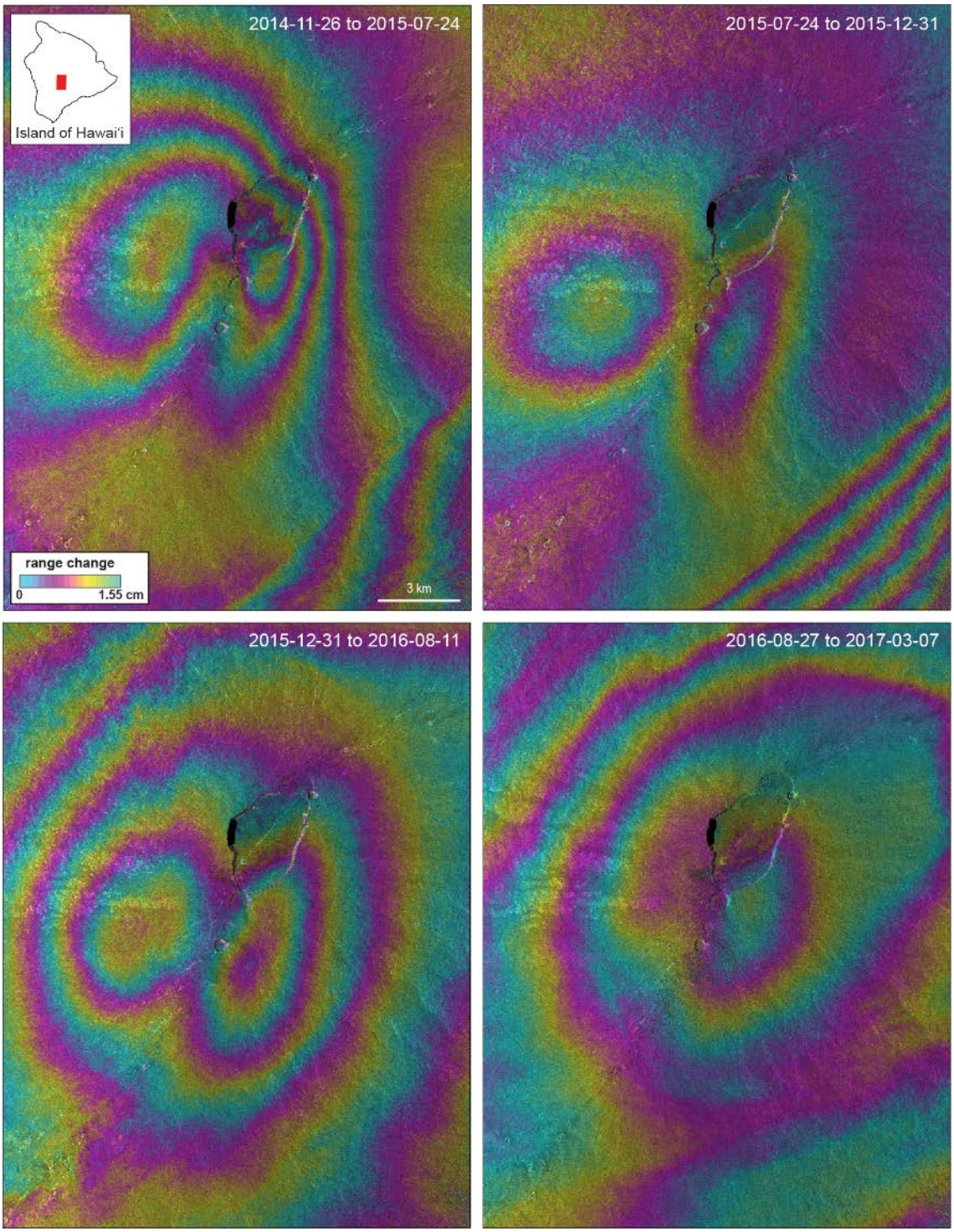

Figure 5. Cosmo_Skymed intereferograms showing inflation of Mauna Loa's summit region during 2014-2017. Note that the locus inflation, defined by the two lobes of line-of-sight inflation, shifts to the southwest during mid-2015 to mid-2016 (upper right and lower left) relatively to early 2015 and late 2016 (upper left and lower right).

GSNL - Geohazard Supersites and Natural Laboratories

Formation of a pit crater on Mauna Kea

On October 16, 2015, a helicopter pilot flying over the south flank of Mauna Kea volcano—which has not erupted in over 4000 years—noticed a new crater within about 1 km of the road accessing the summit of the mountain. Subsequent ground-based observations constrained the new crater to be 24 x 20 m with a depth of 20-35 m (Figure 6). This is the first pit crater known to have formed on Mauna Kea in the past several hundred years.

Figure 6. Worldview images from September 3, 2015 (top) and September 30, 2015 (bottom) showing the new pit crater, which must have formed sometime between the acquisition of the two images. The road to access the summit of Mauna Kea is in the upper left of both images.

RADARSAT-2 data were being automatically acquired over this area and were the only SAR data from any satellite that covered the region and time period of crater formation. The crater was clearly visible in high-resolution of RADARSAT-2 imagery acquired acter September 29, 2015, which further constrained the crater's formation time to be between September 5 and 29, 2015 (Figure 7).

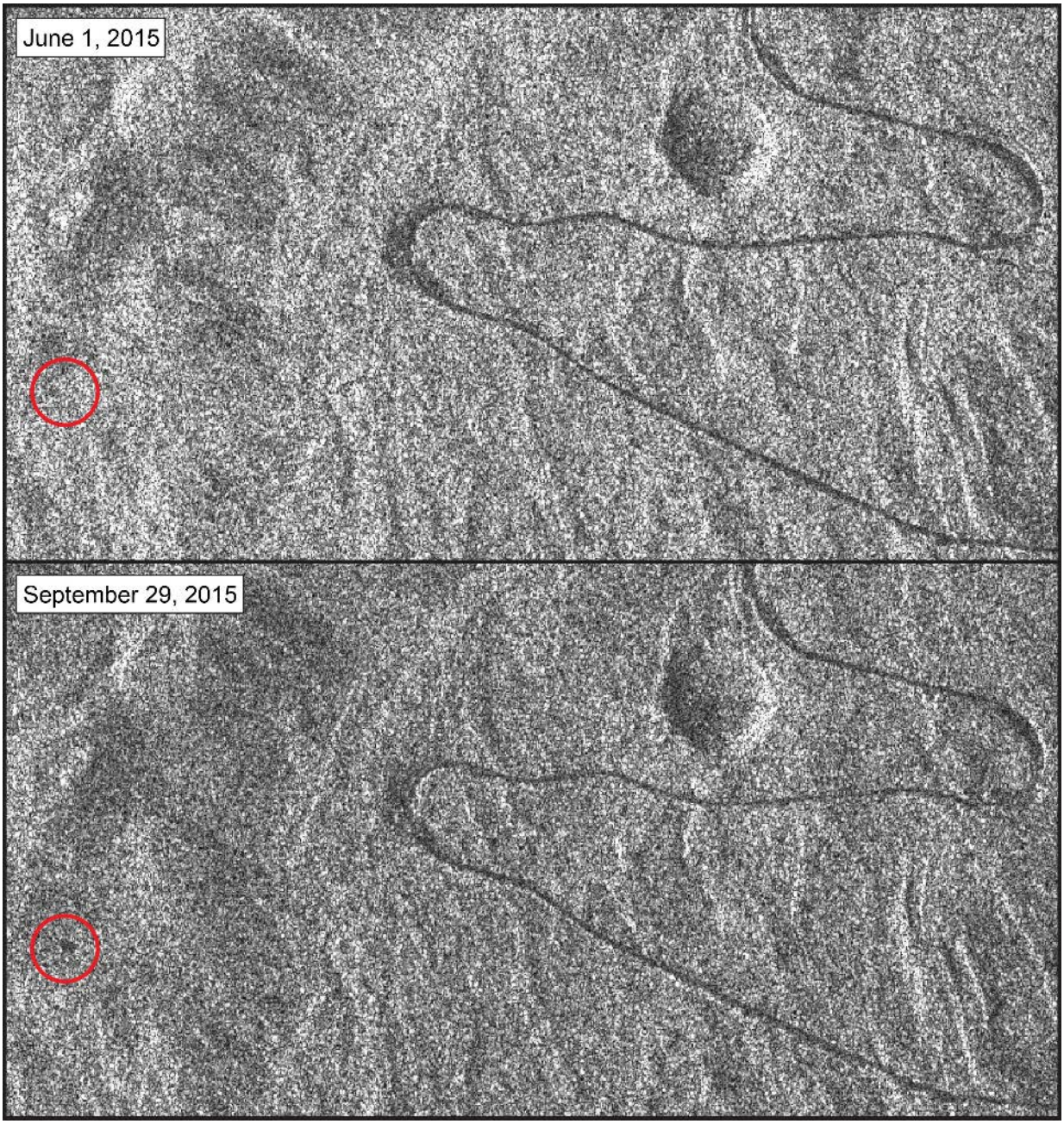

Figure 7. Amplitude imagery from RADARSAT-2 in radar coordinates (i.e., east and west are flipped). Red circle denotes crater location. Dark ribbon in center-left of image is summit access road. Crater is approximately 20 m in diameter.

In addition to constraining the timing of the crater's formation, RADARSAT-2 data suggest the existence of pre-collapse deformation. An examination of the georeferenced interferometric phase for June 1–September 5, 2015 reveals a small area of anomalous phase (Figure 8, top), consistent with about 1 cm of subsidence relative to the surrounding area in the days to weeks before the crater formed. Interferometric phase during September 5–29, 2015, is not coherent at the site of the crater (Figure 8, bottom), as would be expected due to a major change in the scattering properties of the surface. Investigation of this event using satellite SAR would not have been possible without opportunistic RADARSAT-2 acquisitions.

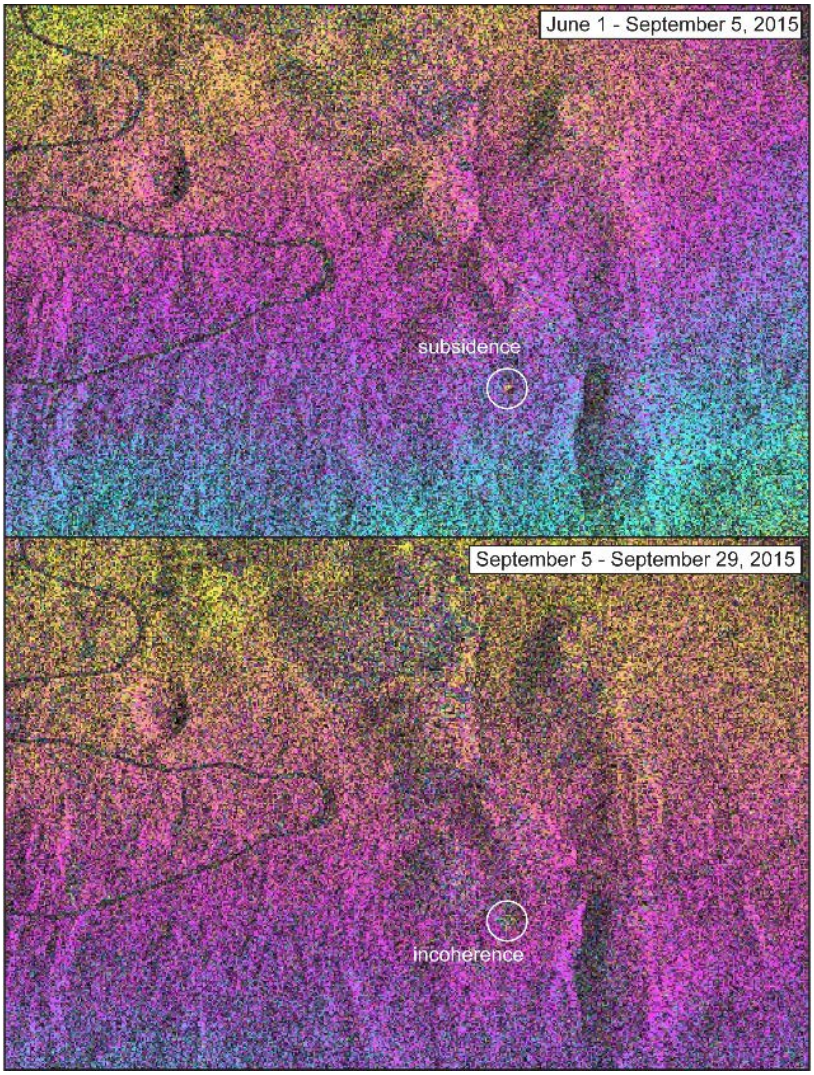

Figure 8. Interferometric phase before (top) and spanning (bottom) formation of the pit crater on the south flank of Mauna Kea. In the images, one fringe is equivalent to 2.8 cm of range change. The pre-collapse interferogram suggests about 1 cm of subsidence at the site of eventual crater formation, while the co-collapse interferogram is incoherent.

May 2015 intrusion at Kīlauea Volcano

A sequence of magmatic events in April-May 2015 at Kīlauea Volcano produced a complex deformation pattern that can be described by multiple deforming sources, active simultaneously. The series of events began on April 22, with rapid inflation of the shallow (~1.5 km below the surface) magma reservoir near Halema‘uma‘u Crater in Kīlauea Caldera (Figure 9). Inflation continued at an exponentially decaying rate for more than a week, while the lava lake within the Halema‘uma‘u eruptive vent rose about 40 m, overtopping its rim and spilling onto the crater floor. Inflation was accompanied by elevated seismicity in the caldera and especially in the upper East Rift Zone. On May 11, borehole tiltmeters began recording rapid deflation of the Halema‘uma‘u reservoir (Figure 10), accompanied by a drop in the level of the lava lake drop and an increase in the rate and magnitude of earthquakes in the south caldera. Within a day, inflation in the south caldera was clear from tilt, GPS and InSAR data. The visual pattern of deformation from InSAR (Figure 11) and simple inverse modeling are consistent with magma accumulation in the south caldera magma reservoir—a complex feature often imaged in the past, especially by leveling and InSAR. Inflation in the south caldera occurred for about 5 days. During this time, the lava lake level continued to drop to about 20 m below pre-April 22 levels. Preliminary modeling suggests that the volume lost from the HMM reservoir and lava lake is comparable to that gained in the south caldera.

This event provides a rare glimpse of rapid magma transfer between two subcaldera magma storage bodies, raising new questions about how these reservoirs are connected and offering the potential to further elucidate the geometry of Kilauea’s summit magma storage system.

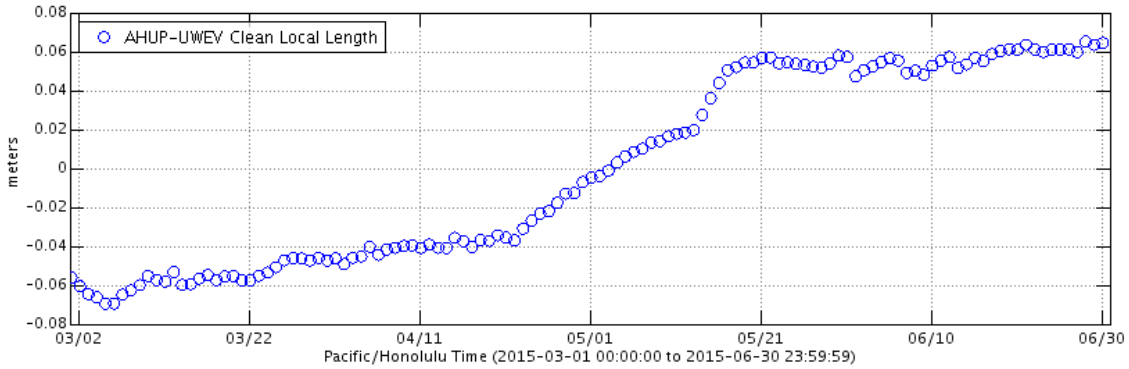

Figure 9. Distance between two GPS stations spanning the summit of Kīlauea Caldera. Positive change is increasing distance, which implies inflation due to subsurface magma accumulation.

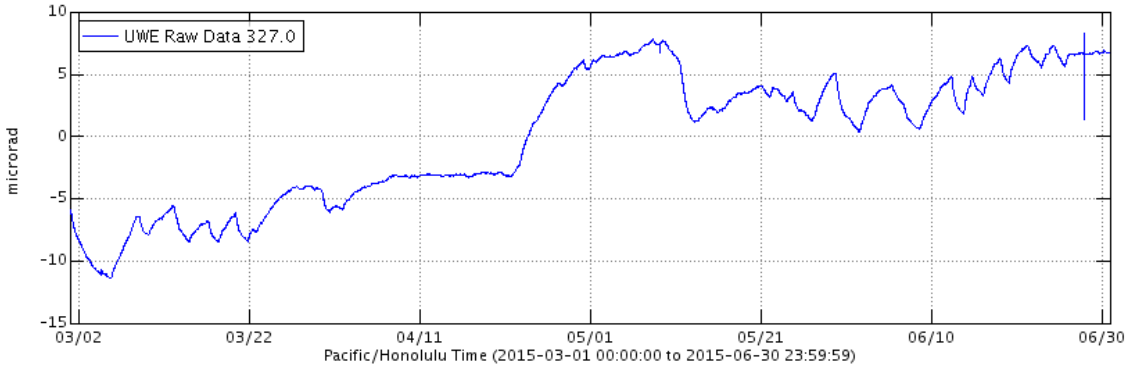

Figure 10. Ground tilt recorded by a borehole instrument located about 2 km northwest of the Halema‘uma‘u lava lake. Positive tilt is away from the caldera (inflation) and negative is toward the caldera (deflation). Rapid deflation on May 11, accompanied by inflation of the south caldera at the same time (Figure 9), indicates drainage of magma from a shallow reservoir beneath Halema‘uma‘u Crater and accumulation of magma in the south caldera.

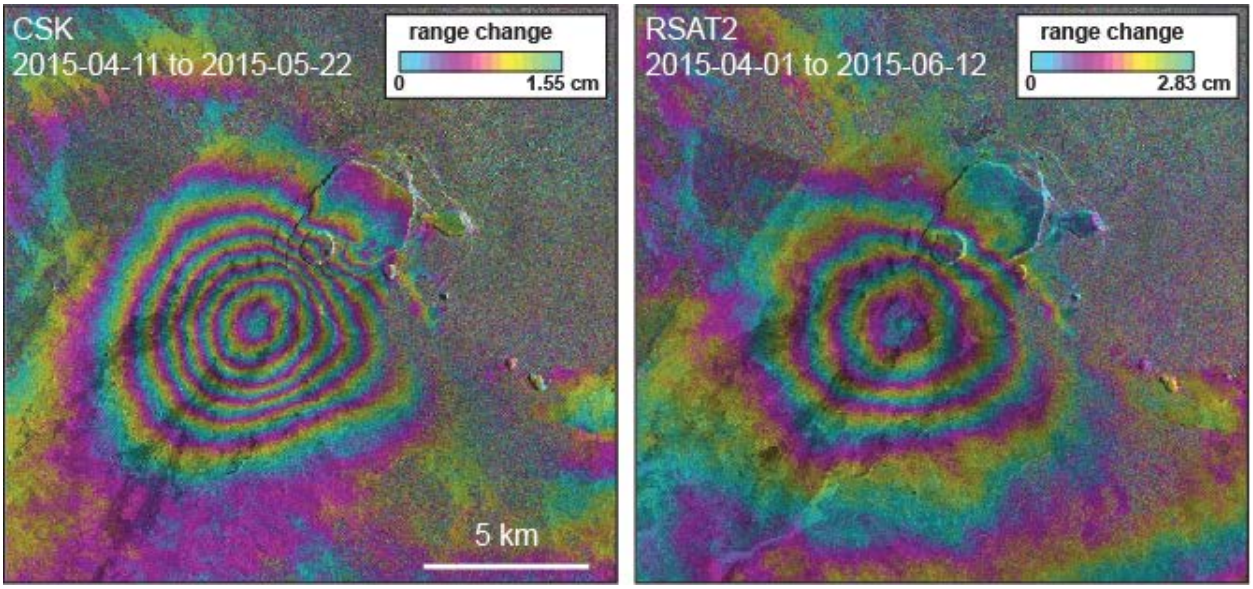

Figure 11. Representative interferograms spanning the April 2015 inflation and May 2015 intrusion at the summit of Kīlauea Volcano from Cosmo-SkyMed (left) and RADARSAT-2 (right).

Increased magma supply to Kīlauea Volcano

A significant recent research result at Kīlauea is documentation of changes in magma supply to the volcano over timescales of years. Magma supply, determined as the combined volume of magma that accumulated beneath the surface and also erupted at the surface, controls the eruptive activity of a given volcano. A surge in supply at Kīlauea during 2003–2007 was associated with the formation of new eruptive vents, while a lull in supply during 2012–2015 was accompanied by sluggish lava flow activity

(which was fortunate, as this may have prevented lava flows from overrunning the village of Pāhoa in late 2014). The changes in magma supply were documented by a combination of datasets, but relied heavily on SAR data. Interferograms were used to assess volumes of magma storage beneath the surface, while changes in surface topography over time derived from TanDEM-X data provided an estimate of eruptive volumes.

A change in eruptive activity in 2016 appears to be associated with the end of the 2012–2015 lull in magma supply. During the lull, eruption rates were on the order of 1-2 m^3/s, and magma storage beneath the surface was negligible (based on models of interferograms). In May-July, 2016, the eruption rate determined from TanDEM-X topographic differences increased to about 4 m^3/s, and interferograms indicated extensive inflation of the summit region (Figure 12), suggesting magma storage—a result that is corroborated by GPS (Figure 13). The inflation plus the increase in lava eruption rates suggests that the magma supply to Kīlauea in 2016 was elevated compared to that of 2012–2015, perhaps suggesting that a change in eruptive activity (e.g., an intrusion or formation of a new eruptive vent) within the coming months is likely.

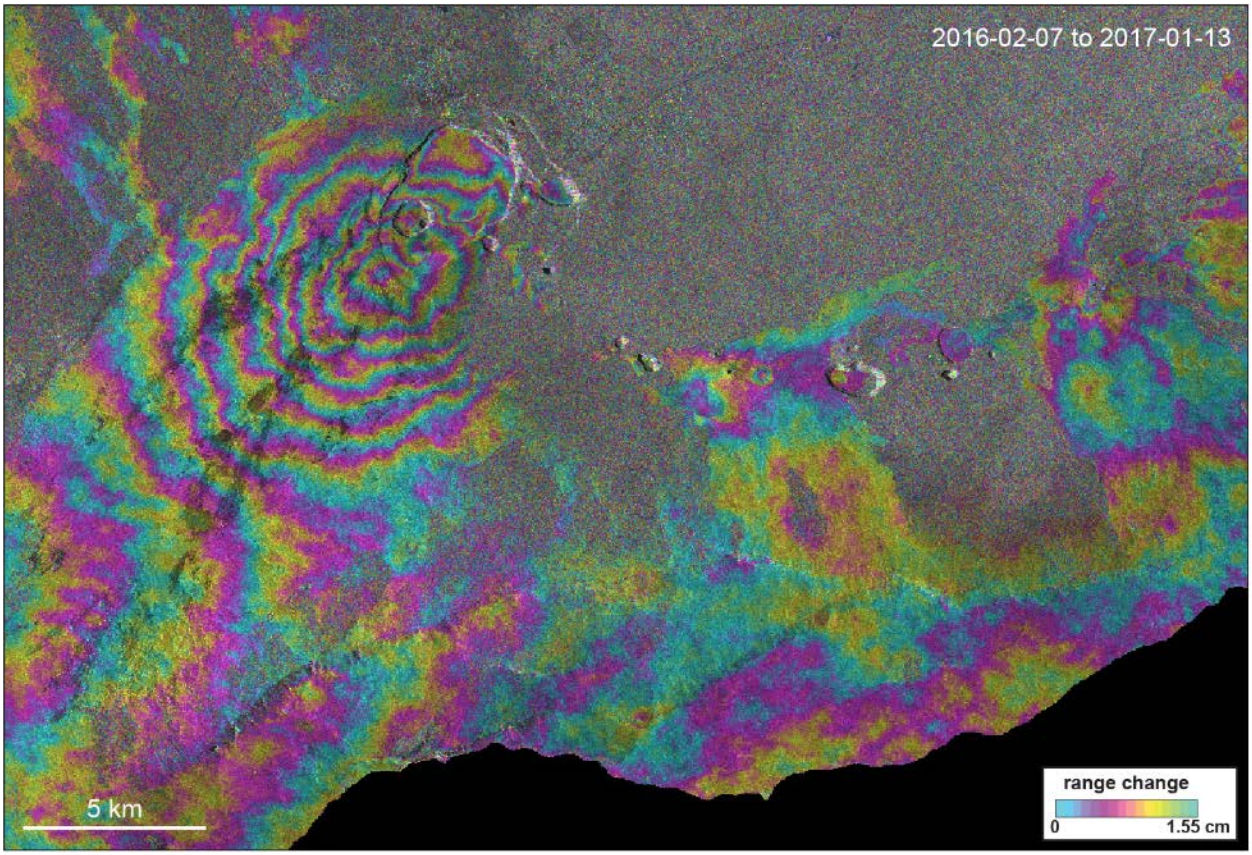

Figure 12. TerraSAR-X interferogram spanning February 7, 2016 to January 13, 2017 and indicating inflation centered in the south part of Kīlauea Caldera.

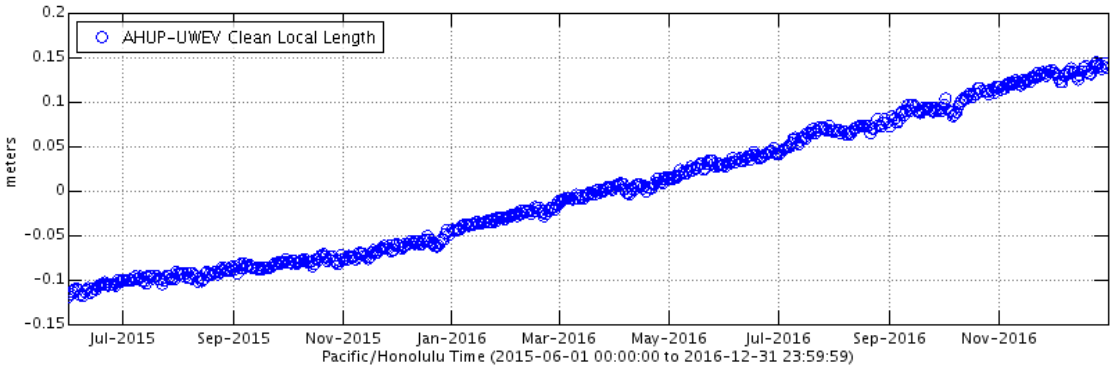

Figure 13. Distance between two GPS stations spanning the summit of Kīlauea Caldera. Positive change is increasing distance, which implies inflation due to subsurface magma accumulation. Inflation of Kīlauea's summit occurred at a relatively steady rate from the May 2015 intrusion through the end of 2016.